JOC The Journal of Organic Chemistry

Article

pubs.acs.org/joc

Curtailing the Hydroxylaminobarbituric Acid–Hydantoin Rearrangement To Favor HNO Generation

Daryl A. Guthrie, Saghar Nourian, Cyrus G. Takahashi, and John P. Toscano*

Department of Chemistry, 3400 North Charles Street, Johns Hopkins University, Baltimore, Maryland 21218, United States

Supporting Information

ABSTRACT: Due to its inherent reactivity, HNO must be generated in situ through the use of donor compounds. One of the primary strategies for the development of new HNO donors has been modifying hydroxylamines with good leaving groups. A recent example of this strategy is the (hydroxylamino)barbituric acid (HABA) class of HNO donors. In this case, however, an undesired intramolecular rearrangement pathway to the corresponding hydantoin derivative competes with HNO formation, particularly in the absence of chemical traps for HNO. This competitive non-HNO-producing pathway has restricted the development of the HABA class to examples with fast HNO release profiles at physiological pH and temperature ($t_{1/2}$ < 1 min). Herein, the factors that favor the rearrangement pathway have been examined and two independent strategies that protect against rearrangement to favor HNO generation have been developed. The timecourse and stoichiometry for the in vitro conversion of these compounds to HNO (trapped as a phosphine aza-ylide) and the corresponding barbituric acid (BA) byproduct have been determined by ^{1}H NMR spectroscopy under physiologically relevant conditions. These results confirm the successful extension of the HABA class of pure HNO donors with half-lives at pH 7.4, 37 °C ranging from 19 to 107 min.

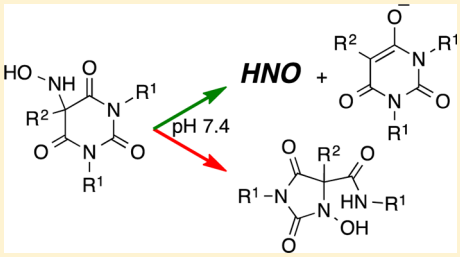

INTRODUCTION

HNO (azanone, nitroxyl) therapy has recently been identified as a potential, alternative treatment for congestive heart failure, a serious condition that is defined as the inability of the heart to pump enough blood to supply the metabolic demands of the body.[1−5] HNO has been shown to improve both vasorelaxation and myocardial contractility via unique mechanisms leading to enhanced intracellular Ca^{2+} cycling.[1] Furthermore, HNO treatment could also expand to alcoholism, vascular dysfunction, and cancer.[2−5]

Limiting these efforts has been the lack of viable HNO donor platforms amenable to structure–activity relationship studies designed to optimize physiochemical and physiological properties. A balance between reactivity and stability is inherent for HNO donors, which are required to be stable enough to store and handle yet reactive enough to evolve HNO under mild conditions (i.e., pH 7.4, 37 °C). As such, HNO evolution from molecular architectures with high reaction potentials is often in competition with alternative, undesired decomposition pathways. Thus, the development of longer-lived HNO donors under physiological conditions has been challenging, as most all HNO donors reported to date have been restricted to examples with fast HNO release profiles with half-lives on the order of a few minutes.

Previously, we have reported three new classes of HNO donors based on the general strategy shown in Scheme 1 for *N*-substituted hydroxylamines where X is a good leaving group: (1) the hydroxylamino-Meldrum's acid (HAMA) class, (2) the (hydroxylamino)barbituric acid (HABA) class, and (3) the (hydroxylamino)pyrazolone (HAPY) class.[6,7] Piloty's acid (PA) and its derivatives, with sulfinate leaving groups, are classic examples of this strategy.[8−12]

Scheme 1. General Strategy for HNO Release and Related Donor Classes

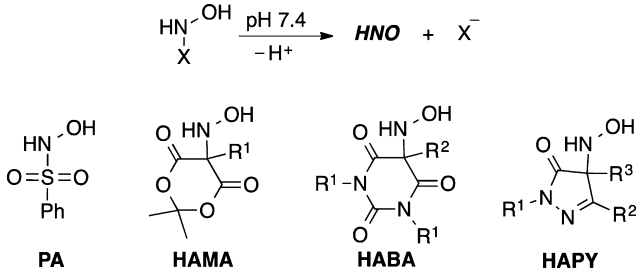

Piloty's acid itself is quite stable at pH 7.4 ($t_{1/2}$ > 1 h) but under physiological conditions can be oxidized, presumably to the corresponding nitroxide, and become an NO donor.[13] To favor deprotonation and HNO formation vs oxidation, electron-withdrawing groups can be attached to the phenyl ring such that the pK_a of the *N*-hydroxysulfonamide precursor is decreased along with an increased stability of the sulfinate leaving group.[9−12]

We have also utilized this strategy with good carbon-based leaving groups such that HNO is released along with a stable carbanion at neutral pH (Scheme 1).[6,7] Like the Piloty's acid class, the HAMA and HABA classes also suffer from alternative

Received: October 12, 2014
Published: January 13, 2015

DOI: 10.1021/jo5023316
J. Org. Chem. 2015, 80, 1349−1356

decomposition pathways, albeit by way of either hydrolysis or an intramolecular rearrangement mechanism, respectively, rather than oxidation. For example, HABA-2 rearranges almost exclusively to the corresponding hydantoin, **1**, with a half-life at pH 7.4, 37 °C of 62 min (Scheme 2). The only reported

Scheme 2. Previous Examples of the HABA Class of Potential HNO Donors

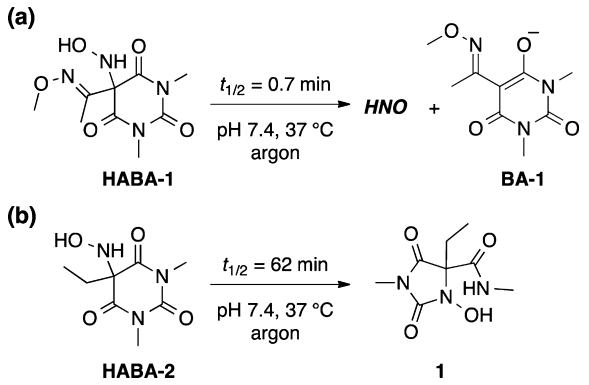

example of a pure HNO donor in this class is HABA-1, which has a short half-life at pH 7.4, 37 °C of 0.7 min.[6] By exchanging the ethyl group in the R^2 position with an *O*-methyloxime, thus creating a more stable carbanion leaving group, HNO production was expedited, and the non-HNO producing rearrangement pathway was avoided. The hydrolysis pathway remains dominant in the corresponding HAMA derivative with *O*-methyloxime substitution.[6] However, the HAPY class is resistant to alternative non-HNO producing mechanisms, and the first series extension of this class is the subject of a companion paper.[7]

Accessing longer lived HNO donors with half-lives on the order of minutes to hours, particularly within the same donor class, is expected to have a broad impact on optimizing HNO release rate for the treatment of any number of potential diseases, including congestive heart failure, alcoholism, vascular dysfunction, and cancer. Furthermore, sustained release of low concentrations of HNO might be an important step to mimic hypothesized endogenous HNO generation.[14] To expand the HABA class of HNO donors, we need to (1) understand what favors the rearrangement pathway and (2) create solutions that minimize or eliminate the possibility of rearrangement.

Herein, we are pleased to report two independent strategies that stabilize the barbituric acid ring against nucleophilic attack by the hydroxylamine functionality to favor HNO generation: (1) exchange of the ethyl group in the R^2 position with a benzyl group for π-interaction with the barbituric acid ring and (2) exchange of the *N*-Me groups in the R^1 positions with *N*-H groups for enol/enolate stabilization of the barbituric acid ring. In both instances, we demonstrate that the non-HNO producing rearrangement pathway becomes kinetically unfavorable, thereby allowing quantitative HNO production under physiologically relevant conditions. Moreover, the benzyl-HABA scaffold is amenable to substitutions on the phenyl ring enabling further optimization of physiochemical and pharmacological properties. We have also prepared such substituted benzyl-HABA compounds with electron-withdrawing and electron-donating groups. Taken together, we have successfully extended the HABA class of pure HNO donors with half-lives ranging from 19 to 107 min under physiologically relevant conditions.

RESULTS AND DISCUSSION

Synthesis. To protect against the hydantoin rearrangement (Scheme 2b), presumably the electrophilicity of the *C*-2 carbon of the barbituric acid ring and/or the nucleophilicity of the hydroxylamine nitrogen must be tempered. We first considered exchanging the ethyl group in the R^2 position with substituted benzyl groups to give HABA-3, HABA-4, and HABA-5 (Table 1). We also considered HABA-6, the 1,3-unsubstituted

Table 1. HNO−Aldol Reaction of Barbituric Acids

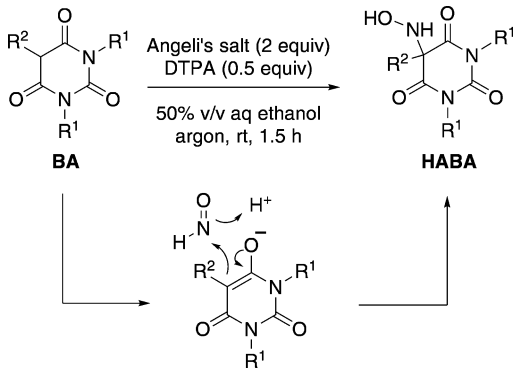

HABA	R^1	R^2	% yield
1	Me	C(=NOMe)Me	45[a]
2	Me	Et	99
3	Me	Bn	99
4	Me	4-OMeBn	99
5	Me	4-ClBn	99
6	H	Et	76

[a]Conversion yield relative to BA-1 determined by ^{1}H NMR.

derivative of HABA-2. These new compounds can be prepared from the corresponding byproducts of HNO release, BA-3−BA-6, which are all known compounds and can be readily prepared (see the Experimental Section).

Taking advantage of the chemical similarity between a nitroso compound and an aldehyde, we have recently developed an HNO−aldol procedure using the HNO donor, Angeli's salt ($Na_2N_2O_3$), as a reagent. This reaction is a variant of the nitroso-aldol reaction[15−17] and is an efficient synthetic route for the HAPY series expansion of HNO donors as well.[7] Likewise, we wanted to apply this procedure to the expansion of the HABA class as well as to the previous examples in this class, HABA-1 and HABA-2. Fortunately, HABA-1−HABA-6 can all be prepared in moderate to excellent yields as shown in Table 1. Moreover, this HNO−aldol procedure is scalable; for example, HABA-3 can be readily prepared on the gram scale under identical concentration and reaction time as the 50 mg scale without loss in isolated yield or product purity.

The lowest yielding example in Table 1 is HABA-1 with a conversion yield of 45%, requiring chromatographic separation from unreacted BA-1. The alternative bromination−displacement−deprotection strategy remains a viable synthetic option for HABA-1 (Scheme 3).[6] For HABA-6, however, only the HNO−aldol strategy is viable due to the inherent acidity of 1,3-unsubsituted barbituric acids. In addition, HABA-2 is efficiently prepared from BA-2 and does not react further to the

DOI: 10.1021/jo5023316
J. Org. Chem. 2015, 80, 1349−1356

Scheme 3. Two Synthetic Pathways to HABA-1

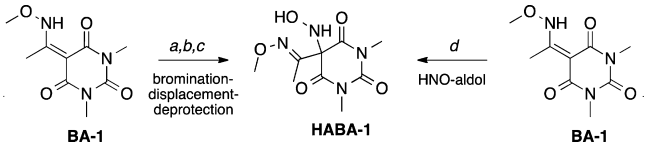

[a]Conditions: TEA, Br_2, CH_2Cl_2, 0 °C, 97%. [b]Conditions: NaH, Boc-NH-O-Boc, DMF, rt. [c]Conditions: AcCl, MeOH, 0 °C to rt, 62% over two steps.[6] [d]See Table 1 for details.

corresponding hydantoin, compound **1**, under the conditions outlined in Table 1.

HNO Release from the Expanded HABA Class. Dimerization of HNO and subsequent dehydration gives nitrous oxide (N_2O).[18] Traditionally, HNO production from a potential HNO donor can be assessed by the analysis of the amount of N_2O formed following donor decomposition. This assay is performed using gas chromatographic headspace analysis of pH 7.4 solutions usually containing a metal chelator, such as diethylenetriaminepentaacetic acid (DTPA), under inert atmosphere to preclude reactivity of HNO with oxygen and trace metals. Like the HAPY series companion paper,[7] this assay is not effective for the measurement of HNO production from the HABA class series extension since the equilibrium favors reactant (HABA) formation, as highlighted in the syntheses of these precursors. Upon examination of HABA-3–HABA-6 relative to the pure HNO donor, HABA-1, only trace to moderate amounts of N_2O are detected following 24 h incubation (Table 2). Thus, an alternative method for the evaluation of HNO production must be utilized.

Table 2. N_2O Headspace Analysis of HABA-3–HABA-6 in pH 7.4 Phosphate Buffer at 37 °C under Argon

HABA	% N_2O[a]
3	12
4	9
5	25
6	0.3

[a]Percent N_2O yield relative to HABA-1 following 24 h incubation.

We have developed an ^{1}H NMR method for the quantification of HNO yields based on a previously reported HPLC method by King and co-workers,[19,20] which utilizes the selective, distinctive, and irreversible trap for HNO, tris(4,6-dimethyl-3-sulfanatophenyl)phosphine trisodium salt (TXPTS).[7] Moreover, this assay can be used to monitor the timecourse and stoichiometry of the HNO donor, the released byproduct, and HNO itself. The reaction scheme for the conversion of HABA-1–HABA-6 to BA-1–BA-6 and HNO (trapped as one molecule of an aza-ylide and one molecule of a phosphine oxide) is shown in Table 3. Importantly, no other organic products arising from compounds HABA-1, HABA-3–HABA-6 are observed. Interestingly, when HABA-2 is incubated in the presence of TXPTS, HNO is now released with its yield comparable with that of the rearrangement product; the yield of the expected byproduct, BA-2, and the HNO-derived TXPTS aza-ylide is 59% relative to the corresponding hydantoin, compound **1**.

This ^{1}H NMR assay utilizes TXPTS in slight excess to render HNO generation from the HABA series irreversible, which occurs at ca. 2 equiv TXPTS for HABA-3 (Figure 1a).

Table 3. Incubation of HABA-1–HABA-6 in pH 7.4 Phosphate Buffer at 37 °C under Argon with Added TXPTS

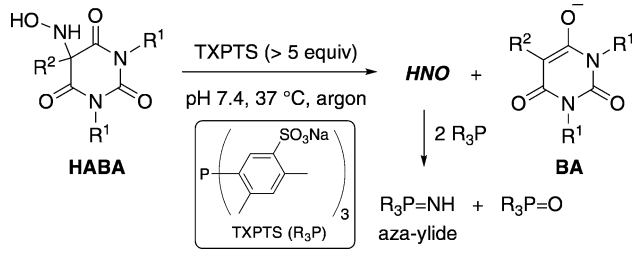

HABA[a]	R^1	R^2	$t_{1/2}$ (min)	k (s^{-1})[b]	% HNO[c]	BA pK_a[d]
1	Me	C(=NOMe)Me	<1	>1.1 × 10^{-2}	99	5.1[e]
2	Me	Et	*f*	*f*	59	4.7
3	Me	Bn	38	3.1 × 10^{-4}	99	4.2
4	Me	4-OMeBn	79	1.5 × 10^{-4}	96	4.3
5	Me	4-ClBn	19	6.0 × 10^{-4}	92	3.7
6	H	Et	107	1.1 × 10^{-4}	97	4.1

[a]Incubation conditions: HABA (1 mM) and TXPTS (5 mM) in 10% D_2O, pH 7.4 phosphate buffer (0.25 M) with DTPA (0.2 mM) at 37 °C under argon. [b]The rates are calculated best fits to a single exponential function of the integrated ^{1}H NMR data for HABA disappearance/BA appearance. [c]HNO yields were determined from the final TXPTS aza-ylide yield. [d]The pK_a values were determined by titration in 50% v/v aqueous ethanol. [e]The pK_a of BA-1 was previously determined in water (pK_a of BA-1 = 4.0).[6] [f]Not determined.

Consistent with the HAPY companion series,[7] these results also indicate no bimolecular, direct reaction between TXPTS and HABA-3, since HABA-3 consumption is not linear with the change in initial [TXPTS]. The complete decomposition of HABA-3 to give BA-3 and the HNO-derived TXPTS aza-ylide under physiologically relevant conditions using the ^{1}H NMR assay described above is shown in Figure 1b, and the decomposition of HABA-3–HABA-6 is shown in Figure 1c.

The acidity of the benzylbarbituric acid byproduct, BA-3, is comparable to benzoic acid. As expected, substituents on the benzyl moiety affect the acidity of the barbituric acid; electron-withdrawing groups increase acidity and electron-donating groups decrease acidity. These substituent effects have been previously demonstrated to obey the Hammett equation on a series of 5-substituted benzyl 1,3-unsubstituted barbituric acid derivatives.[21]

The rates of decomposition of the benzyl derivatives, HABA-3, HABA-4, and HABA-5, correlate with the pK_a values of their respective BA byproducts. As the stability of the resultant carbanion increases, so too does the rate of HNO evolution. The pK_a of the resultant byproducts, BA-3–BA-5, affects the pK_a of the corresponding HABA donors as well, where a sharp increase in observed rate reflects rapid BA formation as a result of HABA deprotonation (Figure 2a). In a similar fashion to the previously studied HAPY class,[7] the decomposition rates reach the time resolution limit (ca. 0.15 s^{-1}) of the UV–vis experiment, precluding a complete pK_a analysis for each donor. Analogously, we believe these results indicate that the barrier to HNO dissociation must be low once deprotonation of the donor occurs.

The longest lived HNO donor in this HABA series is the 1,3-unsubstituted 5-ethyl derivative, HABA-6. As shown in Figure 2b, the ring nitrogen proton is mildly acidic. Contrary to the 1,3-dimethyl derivatives, HABA-3–HABA-5, the pK_a of HABA-

DOI: 10.1021/jo5023316
J. Org. Chem. 2015, 80, 1349–1356

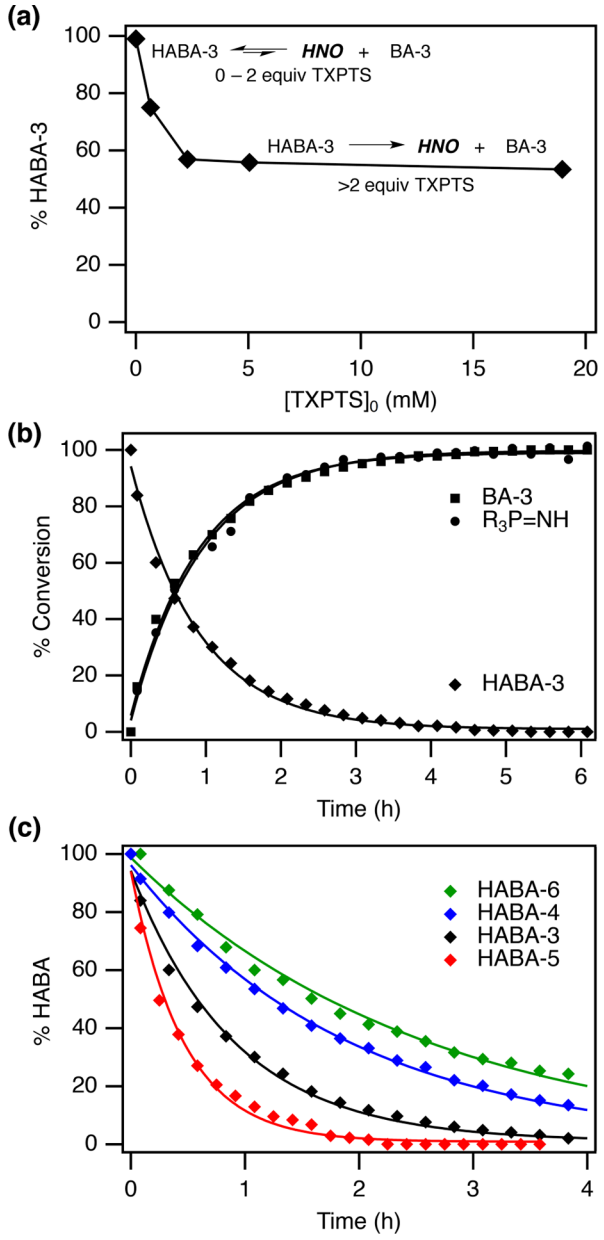

Figure 1. (a) Incubation of HABA-3 at pH 7.4, 37 °C after 40 min as a function of $[TXPTS]_0$. Conditions: HABA-3 (1 mM) in 10% D_2O, pH 7.4 phosphate buffer (0.25 M) with DTPA (0.2 mM) at 37 °C under argon. (b) Timecourse for the disappearance of HABA-3 and appearance of BA-3 and TXPTS aza-ylide with added TXPTS. The solid curves are calculated best fits to a single exponential function of the integrated ^{1}H NMR data ($k = 3.1 \times 10^{-4}$ s^{-1} for each fit). (c) Disappearance of HABA-3 (black), HABA-4 (blue), HABA-5 (red), and HABA-6 (green) under conditions outlined in Table 3.

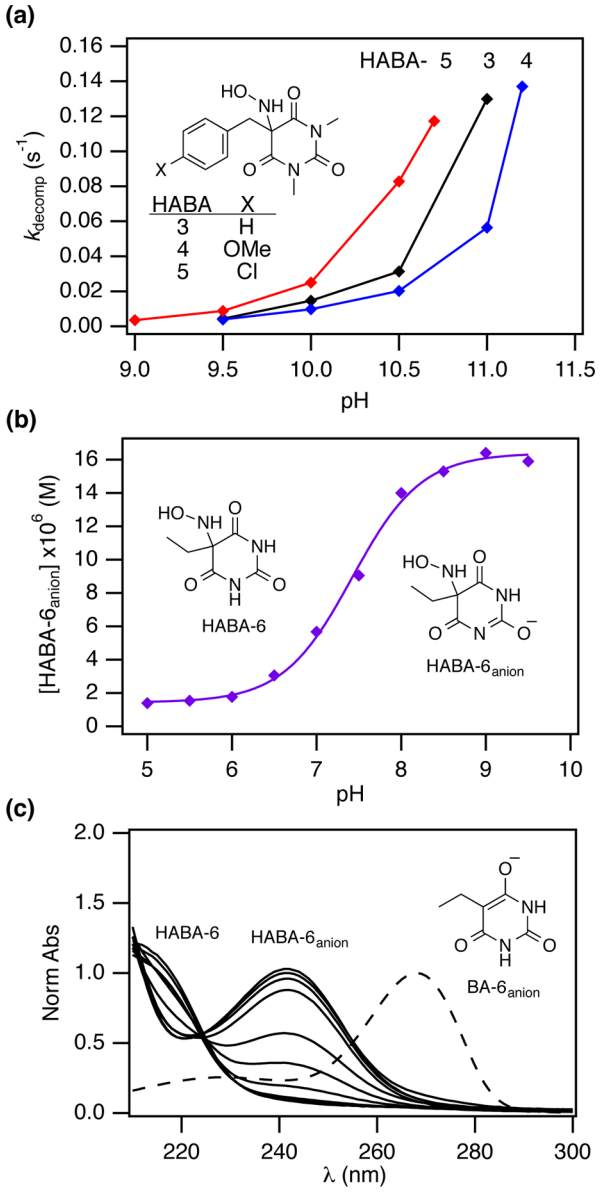

Figure 2. (a) Plot of UV–vis determined decomposition rates as a function of pH at 25 °C for HABA-3 (black), HABA-4 (blue), and HABA-5 (red). (b) Plot of the concentration of HABA-6_{anion} (purple, λ_{max} = 242 nm) as a function of pH. The solid curve is a calculated best fit to a sigmoid function (pK_a = 7.4). (c) Initial UV–vis spectra of HABA-6 from pH 5.0 to 9.5 compared with the expected byproduct of HNO release, BA-6_{anion}, at pH 9.5.

6 as a whole is more acidic with a measured pK_a of ca. 7.4. However, HABA-6 does not rapidly decompose once deprotonated, presumably due to slow *H*OHN–BA-6 deprotonation by the HABA-6_{anion} (Figure 2b) since the difference in acidity of these two positions is expected to be ca. 3–4 pK_a units, based on the pK_a values of the other HABA compounds (Figure 2a).

Figure 2c shows the initial spectra of HABA-6 in a variety of phosphate buffers from pH 5.0 to pH 9.5. As the pH of the buffer increases, a new absorbance at 242 nm is observed, which is consistent with other monoanion 5,5-disubstituted barbituric acids. For example, the λ_{max} of the monoanion of 5,5-diethylbarbituric acid, barbital, is 238 nm.[22] Also, we are confident that the expected byproduct of HNO release, BA-6_{anion}, is not observed in the initial spectra of HABA-6 in any of the buffers and, therefore, does not contribute to the absorbance of HABA-6_{anion} in this UV–vis spectral analysis.

For the HABA class as a whole, HNO release following *H*OHN–BA deprotonation remains the most plausible mechanism in water (Scheme 4), as was the case for the previously studied HAPY class of HNO donors.[7] When R^1 = H (HABA-6), enolate formation on the barbituric acid ring slows the overall rate of HNO generation and inhibits rearrangement (vide infra).

DOI: 10.1021/jo5023316
J. Org. Chem. 2015, 80, 1349–1356

Scheme 4. Mechanism of HNO Release in pH 7.4 Phosphate Buffer at 37 °C

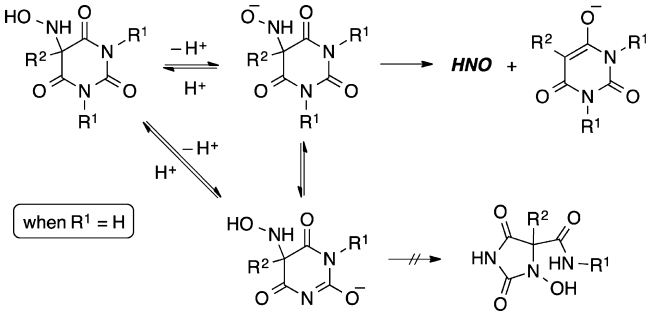

Rearrangement Studies. The aminobarbituric acid–hydantoin rearrangement is a ring contraction of 5-aminobarbituric acids and has been previously studied as a novel method of producing hydantoins, which are important medicinal compounds.[23,24] When the R^1 position is unsubstituted, the rearrangement follows a deprotonation–elimination–addition mechanism (Scheme 5a). However, 1,3-disubstitution prevents the formation of an isocyanate intermediate, and a mechanism involving a carbamate intermediate becomes operative (Scheme 5b). These reactions are performed under forcing conditions (i.e., up to 4 equiv of NaOEt and 120 °C in ethanol for 5 h).

In the same time period, but under much milder conditions (pH 7.4, 37 °C, 5 h), the rearrangement of HABA-2 is complete; the measured half-life is 62 min (Scheme 5c, path A; Figure 3). However, if the *H*OHN–BA-2 hydrogen is replaced with a methyl group (compound **2**, Figure 3) then only approximately 4% of the corresponding rearranged hydantoin

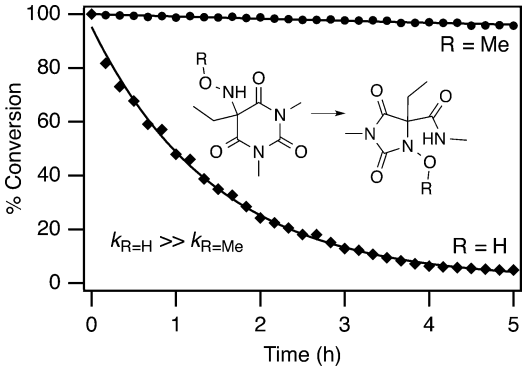

Figure 3. Hydantoin formation from HABA-2 (◆, R = H) vs compound **2** (●, R = Me). For HABA-2, the solid curve is a calculated best fit to a single exponential function of the integrated ^{1}H NMR data ($k = 1.9 \times 10^{-4}$ s^{-1}).

product is observed after 5 h at pH 7.4, 37 °C (Figure 3). Thus, the relatively facile rearrangement of HABA-2 is due in part to the ability of the free *H*OHN–BA-2 hydrogen to activate the barbituric acid ring during the rearrangement, which likely follows a direct nucleophilic addition of the hydroxylamine nitrogen prior to ring contraction rather than formation of a carbamic acid intermediate (Scheme 5b), since no other product or intermediate is observed throughout the rearrangement process for either HABA-2 or compound **2**. On the other hand, this activation is also expected to facilitate *H*OHN–BA deprotonation and HNO production (Scheme 5c, Path B).

Because the barbiturate ring of HABA-6 is approximately 50% anionic in pH 7.4 buffer, the electrophilicity of the *C*-2 carbon is substantially reduced, and attack by the hydroxyl-

Scheme 5. Decomposition of Amino- and Hydroxylaminobarbituric Acids

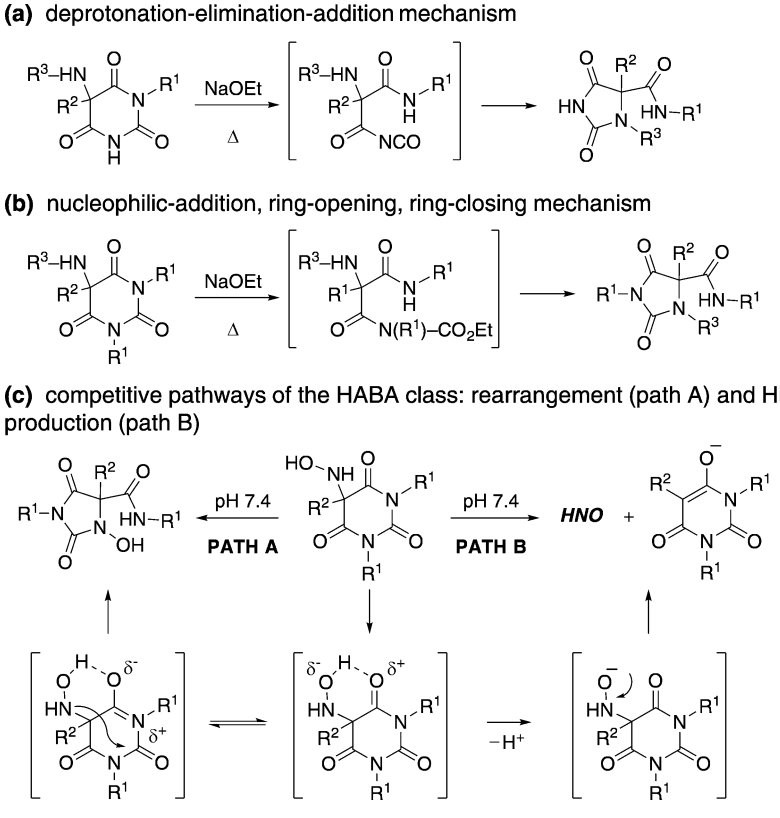

DOI: 10.1021/jo5023316
J. Org. Chem. 2015, 80, 1349–1356

amine nitrogen becomes exceedingly less likely. Ring opening to the corresponding isocyanate intermediate is also evidently not possible (Scheme 5a), since no rearranged product is observed during the decomposition of HABA-6. Even under conditions to disfavor HNO release (i.e., no TXPTS and under argon), the rearranged hydantoin product is not observed even after 2 days of incubation at pH 7.4 and 37 °C in a ^{1}H NMR experiment. In accordance with the negligible N_2O detected from HAPY-6 (Table 2), this compound remained unchanged and is thus relatively stable under these conditions. As with the aminobarbituric acid−hydantoin rearrangement of 1,3-unsubstituted derivatives, the isocyanate intermediate likely requires more forcing conditions for formation.

Similarly, when the benzyl derivative, HABA-3, is incubated under conditions to disfavor HNO release, again in the absence of TXPTS and under argon, the relative rate of rearrangement is substantially slower when compared to the ethyl derivative, HABA-2. After 1 day of incubation at pH 7.4 and 37 °C, the relative ratio of HABA-3/BA-3/hydantoin is 48:16:36. At the same point in time, the BA-3 yield in this ^{1}H NMR experiment is a good match with the N_2O yield from HABA-3 (12%, Table 1). Given the higher rate of HNO release in the presence of a good trap for HNO, such as TXPTS, relative to the rate of rearrangement, the possibility of rearrangement in the substituted-benzyl derivatives is expected to be negligible in vivo, where biological targets for HNO are in excess of HNO.

An explanation as to why rearrangement in the benzyl derivative HABA-3 is so much slower when compared to ethyl derivative HABA-2 is not yet fully understood, since the ability of the free *H*OHN−BA-3 hydrogen to activate the barbituric acid ring during the rearrangement is also possible with HABA-3. Therefore, we employed computational investigations to study the differences between HABA-2 and HABA-3.

A potential explanation for the differences may be due to the ground-state structures of each donor. The lowest energy conformation of HABA-3, both determined computationally and in the crystal structure, is one involving an intramolecular π-interaction, where there is a filled-empty interaction of the HOMO of the phenyl ring with the LUMO of the barbituric acid ring (Figure 4a). Specifically, the dihedral angles of the benzyl group relative to the hydroxylamine in the lowest energy calculated structure and in the crystal structure are 177° and 170°, respectively, thus positioning the two rings in an overlapping conformation (Supporting Information).

For nucleophilic attack of the hydroxylamine nitrogen to occur, this π-interaction must be disrupted to form a tetrahedral intermediate (Figure 4b), which may explain the kinetic unfavorability to rearrangement, as rearrangement to the corresponding hydantoin is thermodynamically favorable for both HABA-2 and HABA-3. Experimentally, the corresponding hydantoin of HABA-2, compound **1**, is stable; even after 1 day at pH 7.4 and 55 °C, compound **1** is unchanged.

Although the calculated tetrahedral intermediates from HABA-2 and HABA-3 are ground-state structures, presumably they are relatively similar in energy to the expected transition state of each reaction. Assuming this is true, the activation barrier to the tetrahedral intermediate (Figure 3b, step 1), is approximately one kcal/mol higher in energy for HABA-3 relative to HABA-2, and the corresponding rate of hydantoin formation is then expected to be 1 order of magnitude slower. In other words, if HABA-2 rearrangement occurs with a half-life of approximately 1 h, a half-life of approximately 10 h is expected for the rearrangement of HABA-3, which is relatively

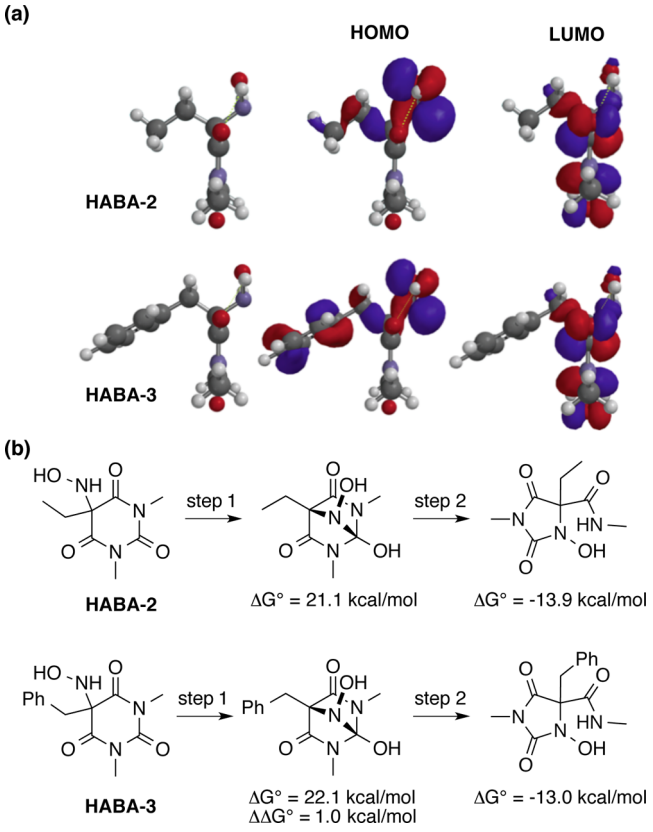

Figure 4. (a) The calculated structures of HABA-2 and HABA-3 and their respective HOMO and LUMO orbital densities. (b) The stepwise scheme and energetics of the rearrangement of HABA-2 and HABA-3 involving a tetrahedral intermediate. All calculations were performed with Spartan '14 at the B3LYP/6-31G* level with an SM8 solvation model for aqueous solvation (Supporting Information).[25]

consistent with our observations concerning the propensity to rearrangement for these two compounds. However, other factors such as steric effects or hydroxylamine nucleophilicity may also be relevant.

CONCLUSION

Compounds HABA-3−HABA-6 are quantitatively converted to BA-3−BA-6 and HNO, trapped as a TXPTS aza-ylide, with a half-life range of approximately 19−107 min in pH 7.4 phosphate buffer at 37 °C. The alternative, undesired rearrangement mechanism that can occur with the HABA class of compounds has been shown to be kinetically unfavorable for this expanded HABA series under physiologically relevant conditions, including the *O*-methylated model compound **2**, which may suggest future prodrug strategies. Another potentially practical benefit enjoyed by the HABA class is that these donors are achiral, removing the need for any study into the differences in physiological effects between enantiomers. We believe these donors will be useful in in vivo studies to evaluate the effects that long-lived, pure HNO donors have on the treatments of any number of potential diseases.

EXPERIMENTAL SECTION

Materials. All starting materials were of reagent grade and used without further purification. Angeli's salt ($Na_2N_2O_3$),[26] HABA-1 and HABA-2,[6] BA-1−BA-6,[6,27,28] *N*-(*tert*-butoxycarbonyl)-*O*-methylhydroxylamine,[29] and 5-bromo-5-ethyl-1,3-dimethylbarbituric acid[6] are

DOI: 10.1021/jo5023316
J. Org. Chem. 2015, 80, 1349−1356

all known compounds and were prepared according to literature procedures. Authentic HABA-1 and HABA-2 were spectral matches to synthetic HABA-1 and HABA-2 via the HNO−aldol procedure. Tris(4,6-dimethyl-3-sulfanatophenyl)phosphine trisodium salt (TXPTS) was of reagent grade and used without further purification. Synthetic TXPTS aza-ylide was obtained through the amidation of TXPTS using hydroxylamine *O*-sulfonic acid in water.[30] Melting point measurements are uncorrected. NMR spectra were obtained on a 400 MHz FT-NMR spectrometer. All chemical shifts are reported in parts per million (ppm) relative to residual $CHCl_3$ (7.26 ppm for ^1H, 77.2 ppm for ^{13}C) or residual DMSO (2.50 ppm for ^1H, 39.5 for ^{13}C). High-resolution mass spectra were obtained on a magnetic sector mass spectrometer operating in fast atom bombardment (FAB) mode. Ultraviolet−visible (UV−vis) absorption spectra were obtained using a diode array spectrometer. Buffered solutions (0.1 M) for UV−vis experiments were prepared from $NaPO_3H_2/Na_2PO_3H/Na_3PO_4$ (pH 5.0, 5.5, 6.0, 6.5, 7.0, 7.5, 8.0, 8.5, 9.0, 9.5, 10.0, 10.5, 10.7, 11.0, 11.2).

^{1}H NMR Incubation Procedure of HABA Donors at pH 7.4, 37 °C with TXPTS. *General Methods.* All ^1H NMR spectra were obtained in pH 7.4 solution containing 0.25 M phosphate buffer, 0.2 mM of the metal chelator diethylenetriaminepentaacetic acid (DTPA) and 10% D_2O on a 400 MHz FT-NMR spectrometer using a 1 s presaturation pulse to suppress the water signal. Each free induction decay was Fourier transformed, phased, and baseline corrected, and integral areas were measured for the *N*-methyl groups of compounds HABA-1−HABA-5 and BA-1−BA-5, the ($-CH_2CH_3$) groups of HABA-6 and BA-6, and the downfield methyl group of TXPTS aza-ylide. The ^1H NMR spectrum of the HNO derived TXPTS aza-ylide product matched that of synthetic TXPTS aza-ylide. The HNO yield from compounds HABA-1−HABA-6 was determined from the final TXPTS aza-ylide yield.

Procedure. The NMR procedure used was based on an HPLC protocol developed by King and co-workers.[19,20] To an argon-purged NMR solution (1.00 mL) containing TXPTS (3.3 mg, 5 mM) was added HABA (10 μL of 100 mM in methanol-d_4) to give 1 mM as the initial concentration of HABA. The solution was briefly mixed, ca. 0.5 mL was transferred to an argon-purged NMR tube, the sample was then internally incubated at 37 °C, and ^1H NMR spectra were collected using a canned pulse sequence, zg2d, modified to include a 1 s presaturation pulse during the relaxation delay. In the case of HABA-1, the decomposition rate is beyond the scope of this ^1H NMR assay, but is presumably as fast, if not faster, than previously measured by UV−vis in the absence of a chemical trap for HNO, such as TXPTS.[6]

Experimental Procedures. *5-(N-Hydroxylamino)-5-(acetyl-O-methoxyoxime)-1,3-dimethylbarbituric acid (HABA-1).* To 5-(acetyl-*O*-methoxyoxime)-1,3-dimethylbarbituric acid (BA-1) (45 mg, 0.2 mmol), Angeli's salt (49 mg, 0.4 mmol), and powdered DTPA (39 mg, 0.1 mmol) under argon at room temperature was added a degassed mixture of 50% v/v aqueous ethanol (1 mL). The reaction was allowed to stir for 1.5 h, diluted with ethanol (>5 mL), and concentrated to dryness in vacuo with minimum heat (<30 °C). The material was then taken up in dichloromethane, filtered through cotton, and concentrated in vacuo to give a product mixture of the title compound and unreacted BA-1; the conversion yield of 45% for HABA-1 was determined by ^1H NMR spectroscopy.

5-(N-Hydroxylamino)-5-ethyl-1,3-dimethylbarbituric Acid (HABA-2). To 5-ethyl-1,3-dimethylbarbituric acid (BA-2) (39 mg, 0.2 mmol), Angeli's salt (49 mg, 0.4 mmol), and powdered DTPA (39 mg, 0.1 mmol) under argon at room temperature was added a degassed mixture of 50% v/v aqueous ethanol (1 mL). The reaction was allowed to stir for 1.5 h, diluted with ethanol (>5 mL), and concentrated to dryness in vacuo with minimum heat (<30 °C). The material was then taken up in dichloromethane, filtered through cotton, and concentrated in vacuo to give the title compound as a white solid (45 mg, 99%).

5-(N-Hydroxylamino)-5-benzyl-1,3-dimethylbarbituric Acid (HABA-3). To 5-benzyl-1,3-dimethylbarbituric acid (BA-3) (1.231 g, 5 mmol), Angeli's salt (1.22 g, 10 mmol), and powdered DTPA (0.983 g, 2.5 mmol) under nitrogen at room temperature was cannulated a degassed mixture of 50% v/v aqueous ethanol (25 mL). The reaction was allowed to vigorously stir for 10 min in order to dissolve all solids followed by normal stirring under a gentle stream of nitrogen for an additional 1.5 h. At that time, precipitation of a white solid was observed. The reaction was then diluted with ethanol (200 mL) and concentrated to dryness in vacuo with minimum heat (<30 °C). The resultant material was then taken up in dichloromethane (3 × 20 mL), filtered through cotton, and concentrated in vacuo to give the title compound as a white solid (1.385 g, 99%). Mp: 155−157 °C. ^1H NMR (400 MHz, $CDCl_3$) δ: 7.26 (m, 3H), 6.96 (m, 2H), 6.28 (d, 1H, J = 3.2 Hz), 4.98 (d, 1H, J = 3.4 Hz, 1H), 3.13 (s, 6H), 3.08 (s, 2H). ^{13}C NMR (100 MHz, $CDCl_3$) δ: 170.0, 150.0, 131.8, 129.2, 129.0, 128.7, 73.6, 42.9, 28.8. HR-MS (FAB): found m/z = 278.11411 (MH^+), calcd for $C_{13}H_{16}N_3O_4$ 278.11408.

5-(N-Hydroxylamino)-5-(4-methoxybenzyl)-1,3-dimethylbarbituric Acid (HABA-4). To 5-(4-methoxybenzyl)-1,3-dimethylbarbituric acid (BA-4) (55 mg, 0.2 mmol), Angeli's salt (49 mg, 0.4 mmol), and powdered DTPA (39 mg, 0.1 mmol) under argon at room temperature was added a degassed mixture of 50% v/v aqueous ethanol (1 mL). The reaction was allowed to stir for 1.5 h, diluted with ethanol (>5 mL), and concentrated to dryness in vacuo with minimum heat (<30 °C). The material was then taken up in dichloromethane, filtered through cotton, and concentrated in vacuo to give the title compound as a white solid (61 mg, 99%). Mp: 108−110 °C. ^1H NMR (400 MHz, $CDCl_3$) δ: 6.88 (d, 2H, J = 8.6 Hz), 6.76 (d, 2H, J = 8.7 Hz), 6.25 (br s, 1H), 5.09 (br s, 1H), 3.76 (s, 3H), 3.15 (s, 6H), 3.03 (s, 2H). ^{13}C NMR (100 MHz, $CDCl_3$) δ: 159.7, 150.1, 130.3, 123.47, 114.3, 73.7, 55.4, 42.1, 28.8. HR-MS (FAB): found m/z = 308.12476 (MH^+), calcd for $C_{14}H_{18}N_3O_5$ 308.12465.

5-(N-Hydroxylamino)-5-(4-chlorobenzyl)-1,3-dimethylbarbituric Acid (HABA-5). To 5-(4-chlorobenzyl)-1,3-dimethylbarbituric acid (BA-5) (56 mg, 0.2 mmol), Angeli's salt (49 mg, 0.4 mmol), and powdered DTPA (39 mg, 0.1 mmol) under argon at room temperature was added a degassed mixture of 50% v/v aqueous ethanol (1 mL). The reaction was allowed to stir for 1.5 h, diluted with ethanol (>5 mL), and concentrated to dryness in vacuo with minimum heat (<30 °C). The material was then taken up in dichloromethane, filtered through cotton, and concentrated in vacuo to give the title compound as a white solid (61 mg, 99%). Mp: 155−157 °C. ^1H NMR (400 MHz, $CDCl_3$) δ: 7.24 (d, 2H, J = 8.5 Hz), 6.91(d, 2H, J = 8.5 Hz), 6.23 (d, 1H, J = 3.3 Hz), 4.98 (d, 1H, J = 3.3 Hz), 3.17 (s, 6H), 3.06 (s, 2H). ^{13}C NMR (100 MHz, $CDCl_3$) δ: 170.0, 149.9, 134.7, 130.6, 130.3, 129.2, 73.1, 41.7, 28.9. HR-MS (FAB): found m/z = 312.07483 (MH^+, ^{35}Cl), 314.07293 (MH^+, ^{37}Cl), calcd for $C_{13}H_{15}ClN_3O_4$ 312.07511 (MH^+, ^{35}Cl), 314.07246 (MH^+, ^{37}Cl).

5-(N-Hydroxylamino)-5-ethylbarbituric Acid (HABA-6). To 5-ethylbarbituric acid (BA-6) (0.781 g, 5 mmol), Angeli's salt (1.22 g, 10 mmol), and powdered DTPA (0.983 g, 2.5 mmol) under nitrogen at room temperature was cannulated a degassed mixture of 50% v/v aqueous ethanol (25 mL). The reaction was allowed to vigorously stir for 10 min in order to dissolve all solids followed by normal stirring under a gentle stream of nitrogen for an additional 1.5 h. The reaction was then diluted with ethanol (200 mL) and filtered through cotton, and the clear filtrate was concentrated to dryness in vacuo with minimum heat (<30 °C). The resultant material was then triturated with diethyl ether and filtered to give the title compound as a light yellow solid (0.707 g, 76%). Mp: >300 °C. ^1H NMR (400 MHz, DMSO-d_6) δ: 11.50 (br s, 2H), 7.95 (s, 1H), 6.23 (s, 1H), 1.66 (q, 2H, J = 7.5 Hz), 0.73 (t, 3H, J = 7.5 Hz). ^{13}C NMR (100 MHz, DMSO-d_6) δ: 172.1, 150.0, 70.9, 26.9, 7.8. HR-MS (FAB): found m/z = 188.06752 (MH^+), calcd for $C_6H_{10}N_3O_4$ 188.06713 (MH^+).

5-(N-(O-Methylhydroxylamino)-5-ethyl-1,3-dimethylbarbituric Acid (2). To a solution of *N*-(*tert*-butoxycarbonyl)-*O*-methylhydroxylamine (0.294 g, 2 mmol) in dimethylformamide (25 mL) at room temperature was added sodium hydride, 60% (0.088 g, 2.2 mmol), and the reaction was stirred for 1 h under nitrogen. To this solution was added 5-bromo-5-ethyl-1,3-dimethylbarbituric acid (0.526 g, 2 mmol), and the reaction proceeded at room temperature for an additional 24 h. The reaction was then diluted with ether (50 mL) and washed with ammonium chloride (×2), water, and brine, dried over magnesium sulfate, filtered, and concentrated in vacuo to give crude 5-(*N*-(*N*-(*tert*-

DOI: 10.1021/jo5023316
J. Org. Chem. 2015, 80, 1349−1356

butoxycarbonyl)-*O*-methyl)hydroxylamino)-5-ethyl-1,3-dimethylbarbituric acid (ca. 50% pure by ^{1}H NMR, contaminated by an unknown product), which was used without further purification. This material was then taken up in dichloromethane (10 mL) and trifluoroacetic acid (10 mL) and allowed to stir at room temperature for 1 h followed by concentration in vacuo to give a mixture of the title compound along with unchanged contaminant. The mixture was dissolved in diethyl ether, diluted with hexanes, and concentrated via rotary evaporation out of the water bath in order to effect precipitation of the unknown product as an off-white solid (0.125 g). The filtrate was concentrated in vacuo to give the title compound (ca. 90% pure by ^{1}H NMR) as a light yellow oil (0.065 mg, 14%). ^{1}H NMR (400 MHz, $CDCl_3$) δ: 5.93 (br s, 1H), 3.49 (s, 3H), 3.38 (s, 3H), 1.87 (q, 2H), 0.82 (t, 3H). ^{13}C NMR (100 MHz, $CDCl_3$) δ: 170.3, 150.9, 71.4, 62.9, 29.7, 29.0, 7.9. HR-MS (FAB): found m/z = 230.11431 (MH^+), calcd for $C_9H_{16}N_3O_4$ 230.11408.

■ ASSOCIATED CONTENT

Supporting Information

Computation results including optimized geometries, energies, and vibrational frequencies and intensities; single-crystal X-ray crystallographic data; NMR spectra. This material is available free of charge via the Internet at http://pubs.acs.org.

■ AUTHOR INFORMATION

Corresponding Author

*E-mail: jtoscano@jhu.edu.

Notes

The authors declare the following competing financial interest(s): J.P.T. is a co-founder and stockholder and serves on the Scientific Advisory Board of Cardioxyl Pharmaceuticals..

■ ACKNOWLEDGMENTS

We gratefully acknowledge the National Science Foundation (CHE-1213438) and Cardioxyl Pharmaceuticals for generous support of this research. We also thank the Johns Hopkins University, Department of Chemistry Facility Managers, Dr. Cathy D. Moore (NMR spectroscopy), Dr. Maxime A. Siegler (single-crystal X-ray crystallography), and Dr. I. Phil Mortimer (HR-MS) for assistance with compound identification and characterization.

■ REFERENCES

(1) Tocchetti, C. G.; Stanley, B. A.; Murray, C. I.; Sivakumaran, V.; Donzelli, S.; Mancardi, D.; Pagliaro, P.; Gao, W. D.; van Eyk, J.; Kass, D. A.; Wink, D. A.; Paolocci, N. *Antioxid. Redox Signal.* **2011**, *14*, 1687−1698.

(2) Flores-Santana, W.; Salmon, D. J.; Donzelli, S.; Switzer, C. H.; Basudhar, D.; Ridnour, L.; Cheng, R.; Glynn, S. A.; Paolocci, N.; Fukuto, J. M.; Miranda, K. M.; Wink, D. A. *Antioxid. Redox Signal.* **2011**, *14*, 1659−1674.

(3) Paolocci, N.; Katori, T.; Champion, H. C.; St. John, M. E.; Miranda, K. M.; Fukuto, J. M.; Wink, D. A.; Kass, D. A. *Proc. Natl. Acad. Sci. U.S.A.* **2003**, *100*, 5537−5542.

(4) Paolocci, N.; Saavedra, W. F.; Miranda, K. M.; Martignani, C.; Isoda, T.; Hare, J. M.; Espey, M. G.; Fukuto, J. M.; Feelisch, M.; Wink, D. A.; Kass, D. A. *Proc. Natl. Acad. Sci. U.S.A.* **2001**, *98*, 10463−10468.

(5) Kemp-Harper, B. K. *Antioxid. Redox Signal.* **2011**, *14*, 1609−1613.

(6) Guthrie, D. A.; Kim, N. Y.; Siegler, M. A.; Moore, C. D.; Toscano, J. P. *J. Am. Chem. Soc.* **2012**, *134*, 1962−1965.

(7) Guthrie, D. A.; Ho, A.; Takahashi, C. G.; Collins, A.; Morris, M.; Toscano, J. P. *J. Org. Chem.* **2015**, DOI: 10.1021/jo502330w.

(8) Bonner, F. T.; Ko, Y. *Inorg. Chem.* **1992**, *31*, 2514−2519.

(9) Toscano, J. P.; Brookfield, F. A.; Cohen, A. D.; Courtney, S. M.; Frost, L. M.; Kalish, V. J. *N*-Hydroxysulfonamide Derivatives as Physiologically Useful Nitroxyl Donors. U.S. Patent US8,030,356, 2011.

(10) Sirsalmath, K.; Suarez, S. A.; Bikiel, D. E.; Doctorovich, F. *J. Inorg. Biochem.* **2013**, *118*, 134−139.

(11) Porcheddu, A.; De Luca, Lidia; Giacomelli, G. *Synlett* **2009**, *13*, 2149−2153.

(12) Aizawa, K.; Nakagawa, H.; Matsuo, K.; Kawai, K.; Ieda, N.; Suzuki, T.; Miyata, N. *Bioorg. Med. Chem. Lett.* **2013**, *23*, 2340−2343.

(13) Zamora, R.; Grzesiok, A.; Weber, H.; Feelisch, M. *Biochem. J.* **1995**, *312*, 333−339.

(14) Choe, C.-U.; Lewerenz, J.; Gerloff, C.; Magnus, T.; Donzelli, S. *Antioxid. Redox Signal.* **2011**, *14*, 1699−1711.

(15) Sandoval, D.; Frazier, C. P.; Bugarin, A.; Read de Alaniz, J. *J. Am. Chem. Soc.* **2012**, *134*, 18948−18951.

(16) Baidya, M.; Griffin, K. A.; Yamamoto, H. *J. Am. Chem. Soc.* **2012**, *134*, 18566−18569.

(17) Palmer, L. I.; Frazier, C. P.; Read de Alaniz, J. *Synthesis* **2014**, *46*, 269−280.

(18) Shafirovich, V.; Lymar, S. V. *Proc. Natl. Acad. Sci. U.S.A.* **2002**, *99*, 7340−7345.

(19) Reisz, J. A.; Klorig, E. B.; Wright, M. W.; King, S. B. *Org. Lett.* **2009**, *11*, 2719−2721.

(20) Reisz, J. A.; Zink, C. N.; King, S. B. *J. Am. Chem. Soc.* **2011**, *133*, 11675−11685.

(21) Tate, J. V.; Tinnerman, W. N., II; Jurevics, V.; Jeskey, H.; Biehl, E. R. *J. Heterocycl. Chem.* **1986**, *23*, 9−11.

(22) Garrett, E. R.; Bojarski, J. T.; Yakatan, G. J. *J. Pharm. Sci.* **1971**, *60*, 1145−1154.

(23) Gütschow, M.; Hecker, T.; Eger, K. *Synthesis* **1999**, 410−414.

(24) Meusel, M.; Ambrożak, A.; Hecker, T.; Gütschow, M. *J. Org. Chem.* **2002**, *68*, 4684−4692.

(25) Shao, Y.; Molnar, L. F.; Jung, Y.; Kussmann, J.; Ochsenfeld, C.; Brown, S. T.; Gilbert, A. T. B.; Slipchenko, L. V.; Levchenko, S. V.; O'Neill, D. P.; DiStasio, R. A., Jr.; Lochan, R. C.; Wang, T.; Beran, G. J. O.; Besley, N. A.; Herbert, J. M.; Lin, C. Y.; Van Voorhis, T.; Chien, S. H.; Sodt, A.; Steele, R. P.; Rassolov, V. A.; Maslen, P. E.; Korambath, P. P.; Adamson, R. D.; Austin, B.; Baker, J.; Byrd, E. F. C.; Dachsel, H.; Doerksen, R. J.; Dreuw, A.; Dunietz, B. D.; Dutoi, A. D.; Furlani, T. R.; Gwaltney, S. R.; Heyden, A.; Hirata, S.; Hsu, C.-P.; Kedziora, G.; Khalliulin, R. Z.; Klunzinger, P.; Lee, A. M.; Lee, M. S.; Liang, W. Z.; Lotan, I.; Nair, N.; Peters, B.; Proynov, E. I.; Pieniazek, P. A.; Rhee, Y. M.; Ritchie, J.; Rosta, E.; Sherrill, C. D.; Simmonett, A. C.; Subotnik, J. E.; Woodcock, H. L., III; Zhang, W.; Bell, A. T.; Chakraborty, A. K.; Chipman, D. M.; Keil, F. J.; Warshel, A.; Hehre, W. J.; Schaefer, H. F.; Kong, J.; Krylov, A. I.; Gill, P. M. W.; Head-Gordon, M. *Phys. Chem. Chem. Phys.* **2006**, *8*, 3172−3191.

(26) King, S. B.; Nagasawa, H. T. *Methods Enzymol.* **1999**, *301*, 211−220.

(27) Jursic, B. S.; Stevens, E. D. *Tetrahedron Lett.* **2003**, *44*, 2203−2210.

(28) Lofberg, C.; Grigg, R.; Keep, A.; Derrick, A.; Sridharan, V.; Kilner, C. *Chem. Commun.* **2006**, 5000−5002.

(29) Kawase, M.; Kitamura, T.; Kikugawa, Y. *J. Org. Chem.* **1989**, *54*, 3394−3403.

(30) Armstrong, A.; Jones, L. H.; Knight, J. D.; Kelsey, R. D. *Org. Lett.* **2005**, *7*, 713−716.

DOI: 10.1021/jo5023316
J. Org. Chem. 2015, 80, 1349−1356